



Xavier University of Louisiana  
**XULA Digital Commons**

---

Faculty and Staff Publications

---

4-2006

## Absolute Magnitude Distributions and Light Curves of Stripped-Envelope Supernovae

D. Richardson

D. Branch

E. Baron

Follow this and additional works at: [https://digitalcommons.xula.edu/fac\\_pub](https://digitalcommons.xula.edu/fac_pub)

 Part of the [Stars, Interstellar Medium and the Galaxy Commons](#)

---

# ABSOLUTE MAGNITUDE DISTRIBUTIONS AND LIGHT CURVES OF STRIPPED-ENVELOPE SUPERNOVAE

DEAN RICHARDSON,<sup>1,2</sup> DAVID BRANCH,<sup>1</sup> AND E. BARON<sup>1</sup>

Received 2005 April 23; accepted 2005 December 9

## ABSTRACT

The absolute visual magnitudes of three Type IIb, 11 Type Ib, and 13 Type Ic supernovae (collectively known as stripped-envelope supernovae) are studied by collecting data on the apparent magnitude, distance, and interstellar extinction of each event. Weighted and unweighted mean absolute magnitudes of the combined sample, as well as various subsets of the sample, are reported. The limited sample size and the considerable uncertainties, especially those associated with extinction in the host galaxies, prevent firm conclusions regarding differences between the absolute magnitudes of supernovae of Types Ib and Ic, and regarding the existence of separate groups of overluminous and normal-luminosity stripped-envelope supernovae. The spectroscopic characteristics of the events of the sample are considered. Three of the four overluminous events are known to have had unusual spectra. Most but not all of the normal-luminosity events have had typical spectra. The light curves of stripped-envelope supernovae are collected and compared. Because SN 1994I in M51 was very well observed, it often is regarded as the prototypical Type Ic supernova, but it has the fastest light curve in the sample. Light curves are modeled by means of a simple analytical technique that, combined with a constraint on  $E/M$  from spectroscopy, yields internally consistent values of ejected mass, kinetic energy, and nickel mass.

*Key words:* stars: evolution — supernovae: general

*Online material:* color figures

## 1. INTRODUCTION

In a recent paper (Richardson et al. 2002, hereafter R02) we carried out a comparative study of the absolute magnitudes of all supernovae (SNe) in the Asiago Catalog. Because of the large number of SNe in the sample, we did not attempt to estimate the extinction of each SN in its host galaxy, and we did not assign uncertainties to individual SN absolute magnitudes. In this paper we look more closely at the absolute magnitude distributions of stripped-envelope supernovae (SE SNe) by assigning uncertainties to each of the quantities that enter into the absolute magnitude determination, including host galaxy extinction. By SE SNe we mean SNe of Types IIb, Ib, and Ic. (The subset containing only SNe Ib and Ic is referred to as SNe Ibc.) The progenitors of SE SNe are stars that have lost most or all of their hydrogen envelopes. This can happen by strong winds such as in Wolf-Rayet stars or through mass transfer to a companion star such as in Roche lobe overflow or a common-envelope phase. The light curves (LCs) of SE SNe are powered by the radioactive decay of  $^{56}\text{Ni}$ , so the absolute magnitudes are closely related to the ejected  $^{56}\text{Ni}$  masses, and in turn to the stellar progenitors and explosion mechanisms. Since the discovery of the apparent association of GRB 980425 with the peculiar Type Ic SN 1998bw (Galama et al. 1999), and the confirmation by spectra of a SN 1998bw–like event associated with GRB 030329 (Garnavich et al. 2003), SE SNe have become of intense interest in connection with gamma-ray bursts (GRBs). Contamination of high-redshift samples of SNe Ia by SE SNe is also an important issue (Homeier 2005).

We also study the  $V$ -band LCs of SE SNe. Data were collected from the literature for two SNe IIb, seven SNe Ib, and 11 SNe Ic, including three that had unusually broad and blue-

shifted absorption features in their spectra (we refer to these as hypernovae). The LCs show considerable diversity in peak brightness, the width of the peak, and the slope of the late-time tail. In order to relate all of the LCs to total ejected mass, ejected nickel mass, and kinetic energy in an internally consistent way, we fitted the data to a simple LC model.

The peak absolute magnitude data and analysis are described in § 2. The LC data and model fits are presented in § 3. A brief summary is given in § 4.

## 2. ABSOLUTE MAGNITUDE DISTRIBUTIONS

### 2.1. Data

R02 worked with the  $B$  band, but for SE SNe the  $V$  band happens to be the one for which most data are available. In order to calculate the peak visual absolute magnitude for each SN, we collected data on the peak apparent visual magnitude, the distance, the foreground Galactic extinction, and the host galaxy extinction, all with assigned uncertainties. We were able to find data for 27 events: three SNe IIb (Table 1), 11 SNe Ib (Table 2), and 13 SNe Ic (Table 3). Eighteen SNe Ibc were in the sample of R02.

#### 2.1.1. Peak Apparent Magnitudes

For most SNe the apparent magnitude and its uncertainty were taken directly from the literature, but in some cases these values were not given, so it was necessary for us to estimate them. For SNe 1998dt, 1999di, and 1999dn we used an uncalibrated  $R$ -band LC (Matheson et al. 2001) together with a calibrated spectrum to determine the peak  $V$  magnitude. We used the spectrum that was nearest to maximum light to calculate the  $R$  magnitude at that epoch and used the  $R$ -band LC to determine the  $R$  magnitude at peak. Then we calculated the  $V - R$  color from the spectrum to determine  $V$  at peak. We examined the available data on  $V - R$  versus time for SNe Ibc and estimated the total uncertainty in  $V$  accordingly. A similar

<sup>1</sup> Department of Physics and Astronomy, University of Oklahoma, Norman, OK 73019.

<sup>2</sup> Physics Department, Marquette University, Milwaukee, WI 53201.

TABLE 1  
ABSOLUTE MAGNITUDE DATA FOR SNe Iib

SN	Galaxy	$V$	Ref.	$\mu^a$	Ref.	$A_V(\text{Galactic})$	$A_V(\text{Host})$	Ref.	$M_V$
1987K.....	NGC 4651	$14.4 \pm 0.3$	1	$31.09 \pm 0.03$	2	$0.088 \pm 0.014$	$0.2 \pm 0.2$	3	$-17.0 \pm 0.4$
1993J.....	NGC 3031	$10.86 \pm 0.02$	4	$27.80 \pm 0.08$	5	$0.266 \pm 0.043$	$0.36 \pm 0.22$	6	$-17.57 \pm 0.24$
1996cb.....	NGC 4651	$13.90 \pm 0.03$	7	$31.09 \pm 0.03$	2	$0.100 \pm 0.016$	$0.10 \pm 0.10$	7	$-17.39 \pm 0.11$

<sup>a</sup> Cepheid-calibrated distance.

REFERENCES.—(1) Filippenko 1988; (2) average of Cepheid distances for NGC 4321, NGC 4535, NGC 4548, and NGC 4639 in the same group (Freedman et al. 2001); (3) Filippenko 1987; (4) van Driel et al. 1993; (5) Freedman et al. 2001; (6) Richmond et al. 1994; (7) Qiu et al. 1999.

method was used for SN 1999cq (Matheson et al. 2000). The peak apparent magnitude for SN 1992ar was taken from Clocchiatti et al. (2000), who, from the limited data available, presented two possible LCs with different peak magnitudes; we adopted the average. In Tables 1–3 we can see that the peak  $V$  magnitudes are the dominant uncertainties in seven cases: the SN Iib 1987K, the SNe Ib 1991D, 1998dt, 1999di, and 1999dn, and the SNe Ic 1992ar and 1999cq.

### 2.1.2. Distances

Distance moduli were, for the most part, obtained as in R02. When possible we used a Cepheid-calibrated distance to the host galaxy or a galaxy in the same group as the host galaxy. The second choice was the distance given in the Nearby Galaxies Catalog (Tully 1988), rescaled from  $H_0 = 75 \text{ km s}^{-1} \text{ Mpc}^{-1}$  to our choice of  $H_0 = 60$  for consistency with R02. We adopted an uncertainty of 0.2 mag in the distance modulus, combined in quadrature with the uncertainty resulting from the radial velocity uncertainty of the host galaxy. One significant change since R02 is that a new distance, based on the tip of the red giant branch, has become available for NGC 4214, the host of SN 1954A (Drozdovsky et al. 2002). We adopt this distance in preference to the (longer) Tully distance used in R02. Now SN 1954A no longer appears to be an overluminous SN Ib. Another change is the distance for SN 1994I. This distance is taken from Feldmeier et al. (1997), who used the planetary nebula luminosity function method. In place of the Tully distance to 1990I, we use the distance given by Elmhamdi et al. (2004), which was obtained by the same method. The uncer-

tainty was estimated by considering the difference between the Tully distance and the Elmhamdi et al. distance. The third choice was the luminosity distance (Kantowski et al. 2000) calculated from the redshift of the host galaxy (in each of these cases  $cz > 2000 \text{ km s}^{-1}$ ) and assuming  $H_0 = 60$ ,  $\Omega_M = 0.3$ , and  $\Omega_\Lambda = 0.7$ . A different choice of  $H_0$  would rescale the absolute magnitudes, and different choices of  $\Omega_M$  and  $\Omega_\Lambda$  would have very small effects on this sample. The uncertainty in the luminosity distance was calculated assuming a peculiar velocity of  $300 \text{ km s}^{-1}$ . For many of the events of our sample, the uncertainty in the distance modulus is significant, although it is dominant only in four cases: SNe 1954A, 1990I, 1997ef, and 1998bw.

### 2.1.3. Extinction

The Galactic extinction is from Schlegel et al. (1998). Values were taken from the NED<sup>3</sup> and converted from  $A_B$  to  $A_V$ . In all cases the uncertainties in the Galactic extinction are comparatively small.

When possible the host galaxy extinction and its uncertainty were taken from the literature. When only the equivalent width of the interstellar Na I D lines,  $W(D)$ , in the host was available we calculated  $E(B - V)$  from the relation  $E(B - V) = 0.16W(D)$  (Turatto et al. 2003) and then used  $A_V = 3.1E(B - V)$ . In this

<sup>3</sup> The NASA/IPAC Extragalactic Database is operated by the Jet Propulsion Laboratory, California Institute of Technology, under contract with the National Aeronautics and Space Administration.

TABLE 2  
ABSOLUTE MAGNITUDE DATA FOR SNe Ib

SN	Galaxy	$V$	Ref.	$\mu$	Ref.	$A_V(\text{Galactic})$	$A_V(\text{Host})$	Ref.	$M_V$
1954A.....	NGC 4214	$9.3 \pm 0.2$	1, 2	$27.13 \pm 0.23$	3	$0.072 \pm 0.012$	$0.05 \pm 0.05$	4	$-17.95 \pm 0.31$
1983N.....	NGC 5236	$11.3 \pm 0.2$	5	$28.25 \pm 0.15^a$	6	$0.228 \pm 0.037$	$0.37 \pm 0.37$	5	$-17.55 \pm 0.45$
1984I.....	E323-G99	$15.98 \pm 0.20$	7	$33.66 \pm 0.20^b$	8	$0.344 \pm 0.055$	$0.05 \pm 0.05$	9	$-18.07 \pm 0.29$
1984L.....	NGC 991	$13.8 \pm 0.2$	10	$31.85 \pm 0.20$	11	$0.091 \pm 0.015$	$0.23 \pm 0.23$	10	$-18.37 \pm 0.36$
1990I.....	NGC 4650A	$15.3 \pm 0.10$	12	$33.30 \pm 0.28$	12	$0.374 \pm 0.060$	$0.13 \pm 0.13$	12	$-18.50 \pm 0.33$
1991D.....	LEDA 84044	$16.4 \pm 0.3$	13	$36.67 \pm 0.05^b$	14	$0.205 \pm 0.033$	$0.05 \pm 0.05$	13	$-20.52 \pm 0.31$
1998dt.....	NGC 945	$17.42 \pm 0.5$	15	$34.45 \pm 0.14^b$	16	$0.085 \pm 0.014$	$0.35 \pm 0.35$	4	$-17.46 \pm 0.63$
1999di.....	NGC 776	$17.91 \pm 0.8$	15	$34.60 \pm 0.13^b$	17	$0.322 \pm 0.052$	$0.67 \pm 0.67$	4	$-17.68 \pm 1.05$
1999dn.....	NGC 7714	$16.48 \pm 0.3$	15	$33.37 \pm 0.23^b$	17	$0.174 \pm 0.028$	$0.05 \pm 0.05$	18	$-17.11 \pm 0.38$
1999ex.....	IC 5179	$16.63 \pm 0.04$	19	$33.80 \pm 0.19^b$	8	$0.067 \pm 0.011$	$1.39 \pm 1.00$	20	$-18.63 \pm 1.02$
2000H.....	IC 454	$17.30 \pm 0.03$	21	$34.11 \pm 0.16^b$	8	$0.760 \pm 0.122$	$0.60 \pm 0.60$	4, 22	$-18.17 \pm 0.63$

<sup>a</sup> Cepheid-calibrated distance.

<sup>b</sup> Luminosity distance ( $H_0 = 60$ ,  $\Omega_M = 0.3$ ,  $\Omega_\Lambda = 0.7$ ; references are for redshifts).

REFERENCES.—(1) Schaefer 1996; (2) Leibundgut et al. 1991 and references therein; (3) Drozdovsky et al. 2002; (4) calculated from the Na I D line; (5) Clocchiatti et al. 1996; (6) Thim et al. 2003; (7) estimated from Leibundgut et al. 1990; (8) NED; (9) Phillips & Graham 1984; (10) Wheeler & Levreault 1985; (11) Nearby Galaxies Catalog (Tully 1988); (12) Elmhamdi et al. 2004; (13) Benetti et al. 2002 and references therein; (14) Maza & Ruiz 1989; (15) estimated from Matheson et al. 2001; (16) Jha et al. 1998; (17) Asiago Catalog (Barbon et al. 1999; <http://web.pd.astro.it/supern/>); (18) Ayani et al. 1999; (19) Stritzinger et al. 2002; (20) Hamuy et al. 2002; (21) Krisciunas & Rest 2000; (22) Benetti et al. 2000.

TABLE 3  
ABSOLUTE MAGNITUDE DATA FOR SNe Ic

SN	Galaxy	$V$	Ref.	$\mu$	Ref.	$A_V(\text{Galactic})$	$A_V(\text{Host})$	Ref.	$M_V$
1962L.....	NGC 1073	$13.13 \pm 0.10$	1	$31.39 \pm 0.20$	2	$0.130 \pm 0.021$	$0.80 \pm 0.80(2)$	3	$-19.19 \pm 0.83$
1964L.....	NGC 3938	$13.6 \pm 0.3$	4	$31.72 \pm 0.14^a$	5	$0.071 \pm 0.011$	$0.56 \pm 0.56(2)$	3	$-18.75 \pm 0.65$
1983I.....	NGC 4051	$13.6 \pm 0.3$	6	$31.72 \pm 0.14^a$	5	$0.043 \pm 0.007$	$0.93 \pm 0.31(5)$	6	$-19.09 \pm 0.45$
1983V.....	NGC 1365	$13.80 \pm 0.20$	7	$31.27 \pm 0.05^a$	8	$0.068 \pm 0.011$	$0.56 \pm 0.22(6)$	7	$-18.10 \pm 0.30$
1987M.....	NGC 2715	$14.7 \pm 0.3$	9	$32.03 \pm 0.23$	2	$0.085 \pm 0.014$	$1.4 \pm 0.6(9)$	10	$-18.82 \pm 0.71$
1990B.....	NGC 4568	$15.75 \pm 0.20$	11	$30.92 \pm 0.05^a$	8	$0.108 \pm 0.017$	$2.63 \pm 1.00(10)$	11	$-17.91 \pm 1.02$
1991N.....	NGC 3310	$13.9 \pm 0.3$	12, 13	$31.84 \pm 0.20$	2	$0.075 \pm 0.012$	$1.0 \pm 1.0(13)$	14	$-19.02 \pm 1.06$
1992ar.....	ANON	$19.54 \pm 0.34$	15	$39.52 \pm 0.01^b$	16	$0.048 \pm 0.008$	$0.25 \pm 0.25(16)$	17	$-20.28 \pm 0.42$
1994I.....	NGC 5194	$12.91 \pm 0.02$	18	$29.62 \pm 0.15$	19	$0.115 \pm 0.018$	$1.4 \pm 0.5(19)$	20	$-18.22 \pm 0.52$
1997ef.....	UGC 4107	$16.47 \pm 0.10$	21	$33.90 \pm 0.18^b$	22	$0.141 \pm 0.022$	$0.05 \pm 0.05(20)$	21	$-17.62 \pm 0.21$
1998bw.....	E184-G82	$13.75 \pm 0.10$	23	$33.13 \pm 0.26^b$	22	$0.194 \pm 0.031$	$0.05 \pm 0.05(23)$	24	$-19.62 \pm 0.28$
1999cq.....	UGC 11268	$16.1 \pm 0.6$	25	$35.64 \pm 0.08^b$	22	$0.180 \pm 0.029$	$0.39 \pm 0.39(24)$	25	$-20.11 \pm 0.72$
2002ap.....	NGC 628	$12.37 \pm 0.04$	26	$30.41 \pm 0.20$	2	$0.161 \pm 0.026$	$0.03 \pm 0.03(26)$	27	$-18.23 \pm 0.21$

<sup>a</sup> Cepheid-calibrated distance.

<sup>b</sup> Luminosity distance ( $H_0 = 60$ ,  $\Omega_M = 0.3$ ,  $\Omega_\Lambda = 0.7$ ; references are for redshifts).

REFERENCES.—(1) Schaefer 1995; (2) Nearby Galaxies Catalog (Tully 1988); (3) estimated from Porter & Filippenko 1987; (4) Leibundgut et al. 1991 and references therein; (5) same group as NGC 3982 (Saha et al. 2001); (6) Tsvetkov 1985; (7) Clocchiatti et al. 1997; (8) Freedman et al. 2001; (9) Filippenko et al. 1990; (10) Nomoto et al. 1990; (11) Clocchiatti et al. 2001; (12) Tsvetkov 1994; (13) Korth 1991a; (14) Grothues & Schmidt-Kaler 1991; (15) Clocchiatti et al. 2000; (16) Phillips & Hamuy 1992; (17) estimated from Clocchiatti et al. 2000; (18) Richmond et al. 1996; (19) Feldmeier et al. 1997; (20) Barth et al. 1996; (21) estimated from Iwamoto et al. 2000; (22) NED; (23) Galama et al. 1998; (24) Nakamura et al. 2001; (25) estimated from Matheson et al. 2000; (26) Gal-Yam et al. 2002 (data actually taken from <http://wise-obs.tau.ac.il/~avishay/local/2002ap/index.html>); (27) Klose et al. 2002.

case we took the uncertainty to be as large as the extinction, up to a maximum uncertainty of 1.0 mag.

The host galaxy extinction for SN 1983V was taken from Clocchiatti et al. (1997). Porter & Filippenko (1987) reported that the H II region associated with SN 1983V was not as prominent as the one associated with SN 1962L but about the same as the one associated with SN 1964L. Having only this information available we assigned the  $A_V(\text{host})$  value of SN 1983V to SN 1964L. For SN 1962L we took the average value of all other SNe Ic in our sample (which is larger than the extinction of SN 1983V). For SNe 1962L and 1964L we assigned an uncertainty as large as the extinction.

For SN 1990B we took the host galaxy extinction from Clocchiatti et al. (2001). They quoted two values, one determined from the Na I D line and one from the color excess; we chose to use the latter. They did not quote an uncertainty except to say that it was large and unknown, so we assigned a large uncertainty of 1.0 mag.

Grothues & Schmidt-Kaler (1991) give the extinction for various regions of NGC 3310, the host galaxy of SN 1991N. Near the position of SN 1991N (Barth et al. 1996) the visual extinction was 1–2 mag, with an uncertainty of about 1 mag. Because the SN was most likely inside rather than behind the H II region, this extinction is probably an overestimate. We adopted  $A_V = 1.0 \pm 1.0$ .

SE SNe tend to be associated with star formation, so they also tend to be significantly extinguished in their host galaxies. Tables 1–3 show that for many events in our sample the uncertainty in the host galaxy extinction is the dominant uncertainty, and overall it is the largest source of absolute magnitude uncertainty for our sample.

## 2.2. Analysis

Absolute visual magnitude is plotted against distance modulus in Figure 1. The slanted dashed line is the line of constant apparent visual magnitude (less the total extinction) of 16. The horizontal dashed line is the SN Ia ridgeline at  $M_V = -19.5$ , shown for comparison. The tendency of intrinsically brighter SNe to be at larger distances, and the fact that all but a few of the

SNe are to the left of the slanted line, are obvious consequences of the strong observational bias in favor of the discovery and follow-up of brighter SNe. The absence of SNe in the lower right part of the figure is a selection effect against lower luminosity events at large distance, and the absence of SNe in the upper left is due to the fact that overluminous events are uncommon, so none happen to have been seen in relatively nearby galaxies. Considering that the events of this sample have been discovered in so many different ways, we make no attempt to correct the absolute magnitude distribution for bias. Instead, we emphasize that in this study we are simply characterizing the available observational sample of SE SNe, a sample in which overluminous events are overrepresented relative to less luminous ones.

In Figure 1 there are quite a few SNe Ic in the distance modulus range from about 29 to 32. There are also quite a few SNe Ib in the distance modulus range from 33 to 35. These groups happen purely by chance. There is no spatial connection, other than distance, between the SNe within each of these groups.

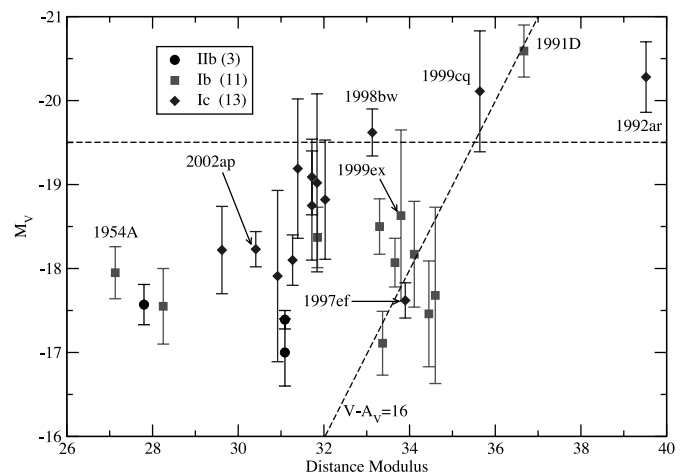


FIG. 1.—Absolute visual magnitude vs. distance modulus with the vertical error bars shown. Some key SNe are labeled. [See the electronic edition of the Journal for a color version of this figure.]

TABLE 4  
MEAN ABSOLUTE MAGNITUDES FOR VARIOUS DATA SETS

DATA SET	WEIGHTED		UNWEIGHTED		N
	$\bar{M}_V$	$\sigma$	$\bar{M}_V$	$\sigma$	
All SE .....	$-18.03 \pm 0.06$	0.89	$-18.40 \pm 0.18$	0.94	27
Bright SE .....	$-20.08 \pm 0.18$	0.46	$-20.13 \pm 0.19$	0.38	4
Normal SE .....	$-17.77 \pm 0.06$	0.49	$-18.10 \pm 0.13$	0.63	23
IIb only .....	$-17.40 \pm 0.10$	0.15	$-17.32 \pm 0.17$	0.29	3
Ib only .....	$-18.37 \pm 0.12$	1.05	$-18.18 \pm 0.27$	0.91	11
Ic only .....	$-18.51 \pm 0.10$	0.86	$-18.84 \pm 0.23$	0.83	13
Normal Ib .....	$-17.98 \pm 0.13$	0.46	$-17.95 \pm 0.16$	0.49	10
Bright Ic .....	$-19.85 \pm 0.22$	0.37	$-20.00 \pm 0.20$	0.34	3
Normal Ic .....	$-18.14 \pm 0.12$	0.48	$-18.49 \pm 0.17$	0.55	10

R02 considered the possibility that SNe Ibc can be divided into two luminosity groups: normal-luminosity SNe Ibc and overluminous SNe Ibc that are even more luminous than SNe Ia. We consider that possibility here also. As can be seen in Figure 1, four events of our sample, three SNe Ic and one SN Ib, are above the SN Ia ridgeline.

The mean absolute magnitude and its standard deviation, both weighted and unweighted, for the whole sample, as well as for several subsets of the sample, are given in Table 4. The weighted mean of the whole sample is  $M_V = -18.03 \pm 0.06$ , with  $\sigma = 0.89$ . When SE SNe are separated into normal-luminosity and overluminous, we have  $M_V = -17.77 \pm 0.06$ ,  $\sigma = 0.49$  for the normal-luminosity events and  $M_V = -20.08 \pm 0.18$ ,  $\sigma = 0.46$  for the overluminous. Comparing the normal-luminosity SNe Ib and Ic, the unweighted means differ by 0.54 mag in the sense that SNe Ic are brighter than SNe Ib, but the weighted means differ by only 0.16 mag, so a difference between normal-luminosity SNe Ib and Ic is not firmly established by these data.

A histogram of the absolute magnitudes is shown in Figure 2. Figure 2 also shows the best Gaussian fit to all of the data, determined by the  $\chi^2$  test using the mean absolute magnitude and dispersion as parameters. The results were  $\bar{M}_V = -18.49$  and  $\sigma = 1.13$ , but the low probability of 15% confirms what is apparent to the eye: the distribution is not adequately fitted by a Gaussian.

Considering the possibility of two luminosity groups, we also fitted the data to a double-peaked distribution. To do this we used

$$f(x) = f_0 \left\{ w \exp \left[ -\frac{(x - x_1)^2}{2\sigma_1^2} \right] + \exp \left[ -\frac{(x - x_2)^2}{2\sigma_2^2} \right] \right\}, \quad (1)$$

with five parameters:  $x_1$  and  $x_2$  (the two mean absolute magnitudes),  $\sigma_1$  and  $\sigma_2$  (the two dispersions), and the weighting factor  $w$ . The normalization factor,  $f_0$ , is equal to  $(1 + w)^{-1}$ . The results for the double-peaked distribution are  $\bar{M}_{V,1} = -20.31$ ,  $\bar{M}_{V,2} = -18.20$ ,  $\sigma_1 = 0.18$ ,  $\sigma_2 = 0.81$ , and  $w = 0.13$ . The probability of this fit is 39%, still quite low.

### 2.3. Comments on Spectra

Here we briefly consider the extent to which SE SNe that have normal luminosities have typical spectra and SE SNe that are overluminous have peculiar spectra.

#### 2.3.1. Type IIb

At early times the spectra of SNe II have conspicuous H $\alpha$  and H $\beta$  P Cygni features, but at later times they resemble the spectra of SNe Ib because the Balmer lines are replaced by He I lines. The early Balmer lines in SN 1996cb are stronger and

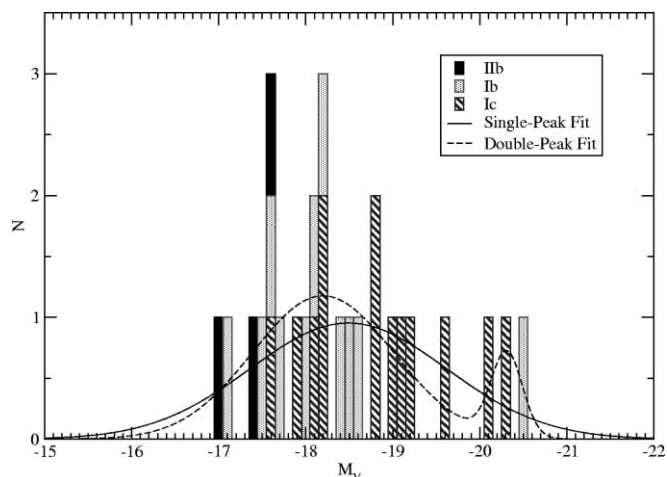


FIG. 2.—Histogram of SE SN absolute magnitudes, with 0.1 mag bin width. The best single-Gaussian and double-Gaussian fits (see text) are also shown. [See the electronic edition of the Journal for a color version of this figure.]

more similar to those of SN 1987A than to those of SN 1993J (Qiu et al. 1999), which may mean that SN 1996cb had a thicker hydrogen layer than SN 1993J. Overall, however, the spectra of the three SN IIb in the sample are rather similar, and the peak absolute magnitudes are the same within the uncertainties.

#### 2.3.2. Type Ib

Branch et al. (2002) studied the optical spectra of a dozen SNe Ib selected on the basis of having deep He I absorption features. The events of that sample displayed a rather high degree of spectral homogeneity, except that three also contained deep H $\alpha$  absorptions. Of the 11 SNe Ib in the present sample, seven were in the sample of Branch et al. (2002): SNe 1983N, 1984L, 1998dt, 1999dn, 1954A, 1999di, and 2000H, with the last three being the “deep-H $\alpha$ ” events. We find that all seven of these events have absolute magnitudes within the normal SN Ib range, and we see no significant difference between the absolute magnitudes of the deep-H $\alpha$  events and the others.

The single available spectrum (Leibundgut et al. 1990) of one of the SNe Ib in our present sample, SN 1984I, covers a limited wavelength range, so that little can be said except that it does appear to be a SN Ib. Its absolute magnitude is within the normal range.

The spectra of SN 1990I contained typical SN Ib absorption features, but they were broader and more blueshifted than those of the Branch et al. (2002) sample (Elmhamdi et al. 2004), although not enough to be considered a hypernova. The absolute magnitude is within the normal range.

SN 1991D has been discussed by Benetti et al. (2002) and Branch (2003). Its He I absorptions were less deep and the velocity at the photosphere near the time of maximum light was lower than in the events of the Branch et al. (2002) sample. Thus, the one overluminous SN Ib of our present sample also had an unusual spectrum.

SN 1999ex was observed by Hamuy et al. (2002), who referred to it as an intermediate Type Ib/c because of its relatively weak He I lines. Branch (2003) refers to it as a “shallow helium” SN Ib because its He I lines were clearly present, although weaker than in the events of the Branch et al. (2002) sample. While this event had an unusual spectrum, according to Table 2 its absolute magnitude is within the normal range.

To summarize SNe Ib: the single overluminous SN Ib of our sample had an unusual spectrum, and most but not all (not SNe

TABLE 5  
SUPERNOVAE WITH LIGHT CURVES

SN	Type	Reference	SN	Type	Reference
1993J.....	I Ib	1, 2, 3	1983I.....	Ic	16
1996cb.....	I Ib	4	1983V.....	Ic	17
1954A.....	I Ib	5, 6, 7	1987M.....	Ic	18
1983N.....	I Ib	8	1990B.....	Ic	19
1984I.....	I Ib	9	1991N.....	Ic	20, 21, 22
1984L.....	I Ib	10	1992ar.....	Ic	23
1990I.....	I Ib	11	1994I.....	Ic	24, 25
1991D.....	I Ib	12	1997ef.....	Ic	26
1999ex.....	I Ib	13	1998bw.....	Ic	27, 28, 29
2000H.....	I Ib	14	2002ap.....	Ic	30, 31, 32
1962L.....	Ic	15			

REFERENCES.—(1) Barbon et al. 1995, <http://web.pd.astro.it/supern/>; (2) van Driel et al. 1993; (3) Lewis et al. 1994; (4) Qiu et al. 1999; (5) Leibundgut et al. 1991; (6) Schaefer 1996; (7) Wellmann & Beyer 1955; (8) Clocchiatti et al. 1996; (9) Leibundgut et al. 1990; (10) Baron et al. 1993 and references therein; (11) Elmhamdi et al. 2004; (12) Benetti et al. 2002; (13) Stritzinger et al. 2002; (14) Krisciunas & Rest 2000; (15) Bertola 1964; (16) Tsvetkov 1985; (17) Clocchiatti et al. 1997; (18) Filippenko et al. 1990; (19) Clocchiatti et al. 2001; (20) Korth 1991a; (21) Korth 1991b; (22) Tsvetkov 1994; (23) Clocchiatti et al. 2000; (24) Clocchiatti et al. 1997; (25) Richmond et al. 1996; (26) Iwamoto et al. 2000; (27) Galama et al. 1998; (28) McKenzie & Schaefer 1999; (29) Sollerman et al. 2000; (30) Foley et al. 2003; (31) Pandey et al. 2003; (32) Yoshii et al. 2003.

1990I and 1999ex) of the normal-luminosity events had normal spectra.

### 2.3.3. Type Ic

Five events of our sample, SNe 1983I, 1983V, 1987M, 1990B, and 1994I, can be said to have had typical SN Ic spectra. The limited available spectra of three others, SNe 1962L, 1964L, and 1991N, also show no indication of peculiarity. The absolute magnitudes of all eight of these events are within the normal SN Ic range.

As is well known, SN 1998bw was overluminous, and its absorption features were very broad and blueshifted. Two other SNe Ic of our sample, SNe 1997ef (Mazzali et al. 2000) and 2002ap (Kinugasa et al. 2002), also had broad spectral features, although not as broad as those of SN 1998bw; these two SNe Ic were *not* overluminous.

Apart from SN 1998bw, the other two overluminous SNe Ic of our sample are SNe 1992ar and 1999cq. Clocchiatti et al. (2000) conclude that the one available spectrum of SN 1992ar is remarkably similar to a spectrum of the Type Ic SN 1983V, which as mentioned above had typical spectra. Matheson et al. (2000) interpret the one good spectrum of SN 1999cq as that of a SN Ic but with unusual (so far unique) narrow lines of He I superposed. The spectrum of SN 1999cq certainly is peculiar.

SN 1999as probably is the brightest SN Ic known, with an absolute magnitude brighter than  $-21.4$  (Hatano et al. 2001), but since no peak apparent magnitude is available, it is not included in our present sample. Its spectrum was quite unusual.

Summarizing SNe Ic: two of the three overluminous events (or three of four, counting SN 1999as) are known to have had unusual spectra. Most but not all (not SNe 1997ef and 2002ap) normal-luminosity events had typical SN Ic spectra.

## 3. LIGHT CURVES

### 3.1. Data

LC data in the *V* band were found for most of the SNe in the absolute magnitude sample of § 2. For a few events, only *R*-band or unfiltered LC data were available. The LC data for many of

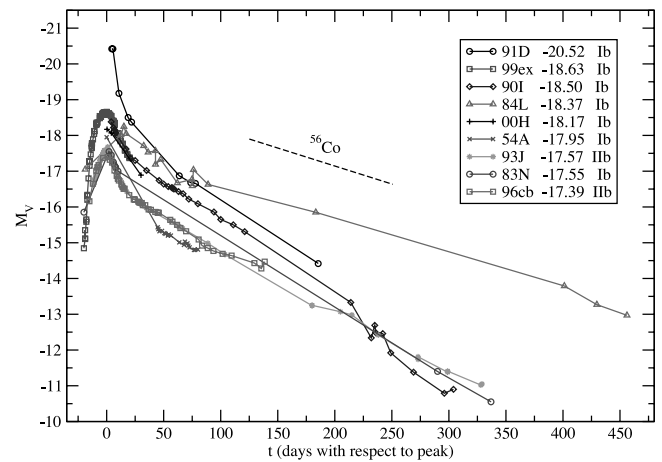


FIG. 3.—Absolute LCs for SNe I Ib and Ib. The peak absolute magnitudes are given in the legend. The  $^{56}\text{Co}$  decay slope is shown for reference. Solid lines are only to guide the eye. [See the electronic edition of the Journal for a color version of this figure.]

the SNe were available from the same reference as the peak magnitude. In some cases we collected data from several sources in order to get as much coverage as possible. For example, most of the data for SN 1994I were taken from Richmond et al. (1996), but two late-time data points were added from Clocchiatti et al. (1997). The SNe that have *V*-band LCs, with references, are listed in Table 5.

The LC data for SNe I Ib/Ib and Ic are shown in Figures 3 and 4, respectively. The lines connect the symbols for each SN to help distinguish the data of one SN from another, but in some cases do not depict the true shapes of the LCs.

The tails of SE SNe are powered primarily by the deposition of gamma rays generated in the decay of  $^{56}\text{Co}$ . Because gamma rays increasingly escape, the slopes of the LCs are steeper than the  $^{56}\text{Co}$  decay slopes. The only exception in the sample is SN 1984L, which has a slow late-time decay slope (Fig. 3).

Figures 5 and 6 are like Figures 3 and 4, respectively, except for covering a shorter time interval in order to show more detail around the time of peak brightness. The two SNe I Ib LCs shown here are very similar and are less luminous than for most SNe Ibc. Exceptional among the SNe I Ib is the extremely luminous SN 1991D, which declined rapidly after peak. SN 1994I was very

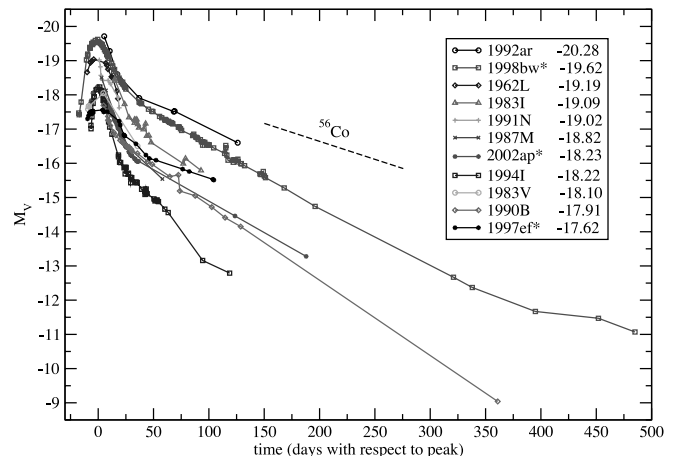


FIG. 4.—Absolute LCs for SNe Ic. The peak absolute magnitudes are given in the legend. The  $^{56}\text{Co}$  decay slope is shown for reference. Solid lines are only to guide the eye (asterisks signify hypervolcanoes). [See the electronic edition of the Journal for a color version of this figure.]

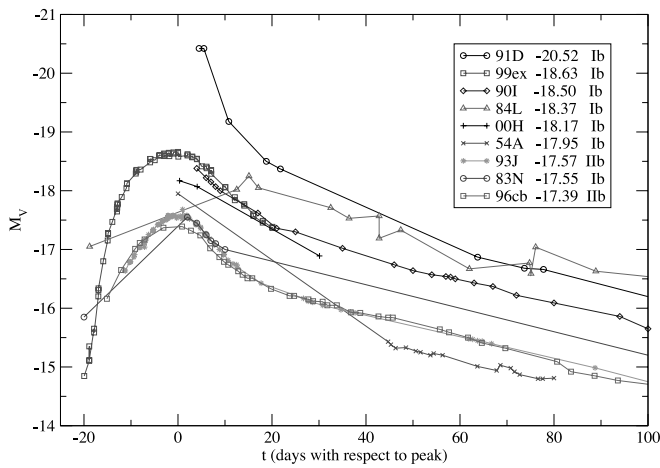


FIG. 5.—Same as Fig. 3, but on a smaller timescale around peak brightness. [See the electronic edition of the Journal for a color version of this figure.]

well observed, and therefore is often regarded as the prototypical SN Ic, but it has the narrowest peak and the fastest overall decline among the SNe Ic of our sample. Model fits for all of the LCs are shown in § 3.2 except for SNe 1954A, 1984I, 1991N, and 2000H because the coverage in their visual LCs was too poor.

### 3.2. The Model

Numerical LC calculations based on hydrodynamic explosion models and various assumptions have been calculated by several groups and compared to the LCs of selected SE SNe. Here we take the approach of adopting a simple analytical model and applying it to all of the SE SNe in our sample. This results in an internally consistent set of explosion parameters (ejected mass, ejected nickel mass, and kinetic energy) for all events. The model is simple, but in view of the evidence that SE SNe tend to be aspherical, most of the numerical LC calculations are also oversimplified.

We use the model of Arnett (1982) for the peak of the LC and the model of Jeffery (1999) for the tail. The Arnett model applies at early times when the diffusion approximation is valid, and the Jeffery model applies at later times when the deposition of gamma rays dominates the LC. As depicted in Figure 7, our model LC switches abruptly from the Arnett LC to the Jeffery LC when the two LCs cross. The underlying assumptions are

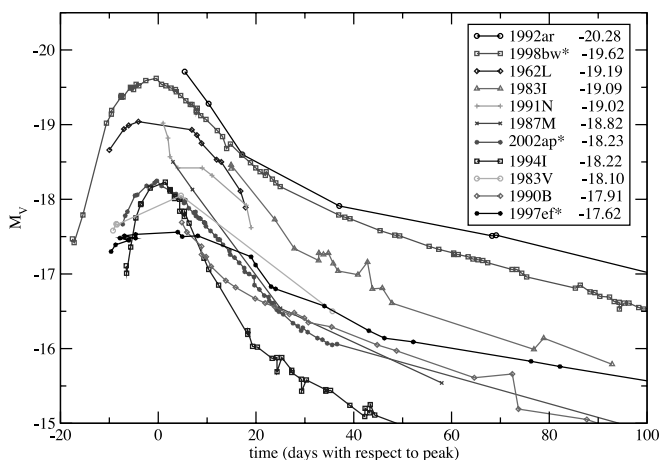


FIG. 6.—Same as Fig. 4, but on a smaller timescale around peak brightness (asterisks signify hypernovae). [See the electronic edition of the Journal for a color version of this figure.]

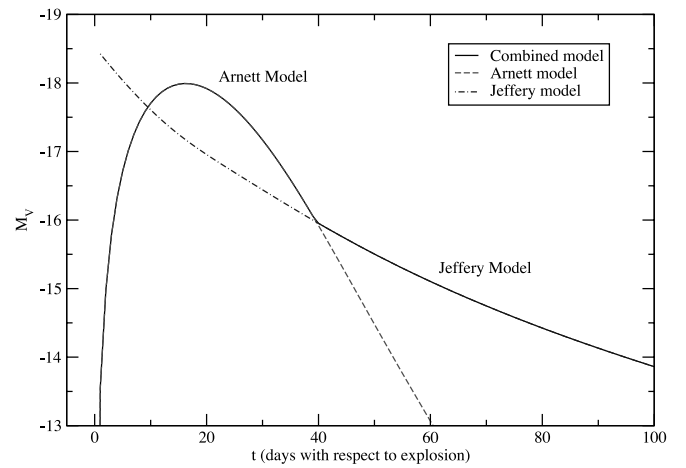


FIG. 7.—Combined model (solid line) and Arnett and Jeffery models (dashed lines). [See the electronic edition of the Journal for a color version of this figure.]

poorest at the time of the transition. The basic assumptions are spherical symmetry; homologous expansion; that  $^{56}\text{Ni}$  is centrally concentrated rather than mixed outward in the ejecta; radiation-pressure dominance at early times; constant optical opacity at early times; and constant gamma-ray opacity at late times. The luminosity of the Arnett part is

$$L_A(t) = \epsilon_{\text{Ni}} M_{\text{Ni}} 10^{-\zeta/2.5} e^{-x^2} \int_0^x 2ze^{-2zy+z^2} dz, \quad (2)$$

where  $x \equiv t/\tau_m$ ,  $y \equiv \tau_m/2t_{e,\text{Ni}}$ ,

$$\tau_m = \sqrt{\frac{\kappa_{\text{opt}}}{\beta c} \sqrt{\frac{6M_{\text{ej}}^3}{5E_k}}}, \quad (3)$$

$$\epsilon_{\text{Ni}} = \frac{Q_{\text{ph+PE}}^{\text{Ni}}}{m_{\text{Ni}} t_{e,\text{Ni}}}. \quad (4)$$

The luminosity of the Jeffery part is

$$L_J(t) = \epsilon_{\text{Ni}} M_{\text{Ni}} \left\{ e^{-t/t_{e,\text{Ni}}} + G \left( e^{-t/t_{e,\text{Co}}} - e^{-t/t_{e,\text{Ni}}} \right) \times \left[ f_{\text{PE}}^{\text{Co}} + f_{\text{ph}}^{\text{Co}} \left( 1 - e^{-(t_0/t)^2} \right) \right] \right\}, \quad (5)$$

where

$$t_0 = \sqrt{\frac{M_{\text{ej}} \kappa_{\gamma}}{4\pi v_a v_b}}, \quad (6)$$

$$v_i = v_i^{93J} \sqrt{\frac{E_k/M_{\text{ej}}}{(E_k/M_{\text{ej}})_{93J}}}, \quad i = a, b, \quad (7)$$

$$G = \left( \frac{Q_{\text{ph+PE}}^{\text{Co}}}{Q_{\text{ph+PE}}^{\text{Ni}}} \right) \left( \frac{m_{\text{Ni}}}{m_{\text{Co}}} \right) \left( \frac{t_{e,\text{Ni}}}{t_{e,\text{Co}} - t_{e,\text{Ni}}} \right) = 0.184641. \quad (8)$$

The  $e$ -folding times for  $^{56}\text{Co}$  and  $^{56}\text{Ni}$  decay,  $t_{e,\text{Co}}$  and  $t_{e,\text{Ni}}$ , are 111 and 8.77 days, respectively. The energies per decay, including energy from photons and electron-positron pairs but

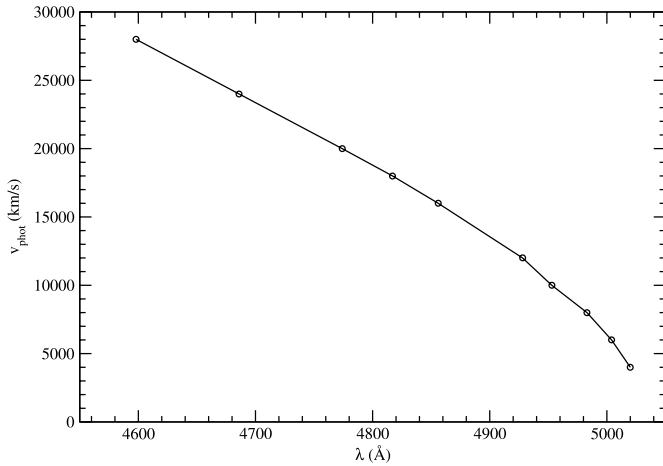


FIG. 8.—Relation between  $v_{\text{phot}}$  and the peak of the Fe II blend near 5000 Å as determined by SYNOW.

not from neutrinos (which escape), are  $Q_{\text{ph+PE}}^{\text{Co}} = 3.74$  MeV and  $Q_{\text{ph+PE}}^{\text{Ni}} = 1.73$  MeV. For  $^{56}\text{Co}$  decay the fractions of energy in photons  $f_{\text{ph}}$  and in the kinetic energy of positrons  $f_{\text{PE}}$  are 0.968 and 0.032, respectively. The above quantities are from Table 1 of Jeffery (1999). The optical and gamma-ray opacities are taken to be  $\kappa_{\text{opt}} = 0.4 \text{ cm}^2 \text{ g}^{-1}$  and  $\kappa_{\gamma} = 0.04 \text{ cm}^2 \text{ g}^{-1}$ . Arnett (1982) defined  $\beta$  as  $4\pi(\alpha I_M/3)$ , where  $\alpha I_M = 3.29$  for uniform density (Arnett 1980).

The model LC is bolometric.  $V$ -band LCs are generally regarded as having similar shape, but in order to adjust the brightness of the model to better match a  $V$ -band LC, a correction  $\zeta$

was used for the Arnett part of the LC. The value of  $\zeta$  was determined by calibrating the peak of the LC to that of a typical SN Ia. This was done by fixing  $E_k$  to 1 foe ( $10^{51}$  ergs),  $M_{\text{ej}}$  to  $1.4 M_{\odot}$ , and  $M_{\text{Ni}}$  to  $0.6 M_{\odot}$ , then choosing  $\zeta = -1.48$  so that the peak absolute magnitude became  $-19.5$ .

The velocities  $v_a$  and  $v_b$  are the inner and outer velocities within which the mass density can be regarded as roughly constant. Jeffery (1999) used velocities thought to be appropriate for SN 1987A. A better approximation for SE SNe is to use velocities thought to be appropriate for SN 1993J (the most thoroughly observed and modeled SE SN) and to rescale these velocities with respect to  $E_k/M_{\text{ej}}$  for each SN (eq. [7]). For SN 1993J we use  $v_a = 1000 \text{ km s}^{-1}$ ,  $v_b = 10,000 \text{ km s}^{-1}$ , and  $(E_k/M_{\text{ej}})_{93J} = 0.51 \text{ foe } M_{\odot}^{-1}$ , from Blinnikov et al. (1998).

We began our study with four adjustable model parameters:  $E_k$ ,  $M_{\text{ej}}$ ,  $M_{\text{Ni}}$ , and  $t_{\text{shift}}$ , where  $t_{\text{shift}}$  shifts the LC on the time axis. The best  $\chi^2$  fit often was formally very good, but the model parameters were physically unreasonable. To remedy this problem we developed the following procedure for constraining the  $E_k/M_{\text{ej}}$  ratio using spectroscopic information. We used the parameterized SN synthetic spectrum code SYNOW (Branch et al. 2002) to construct a relation between the wavelength of the peak of an Fe II blend near 5000 Å and the SYNOW input parameter  $v_{\text{phot}}$ , the velocity at the photosphere (Fig. 8). We measured the wavelength of the peak in the spectra of each event and obtained a value of  $v_{\text{phot}}$  from Figure 8. We defined  $a(t) = (E_k/M_{\text{ej}})/v_{\text{phot}}^2(t)$  and used values of  $E_k/M_{\text{ej}}$  obtained by others from numerical LC calculations for seven events of our sample (references are in Table 6) to construct Figures 9 and 10 for normal-luminosity SE SNe and hypernovae, respectively. In these figures the dashed line is the adopted relation, and the

TABLE 6  
PARAMETERS OF THE BEST LIGHT-CURVE FITS

SN	$E_k$ (foe)	Ref.	$M_{\text{ej}}$ ( $M_{\odot}$ )	$M_{\text{Ni}}$ ( $M_{\odot}$ )	$t_{\text{rise}}$ (days)	$\chi_r^2$	$\delta M_V$ (mag)	$N$
IIb								
1993J.....	0.66	1	1.3	0.10	20	2.14	0.26	89
1996cb.....	0.22	2	0.9	0.08	20	1.30	0.18	44
Ib								
1983N.....	0.30	3	0.8	0.10	18	2.27E-2	0.45	9
1984L.....	2.16	2	4.0	0.92	27	2.63	0.91	17
1984L pk.....	0.97	2	1.8	0.37	22	0.144	0.91	17
1990I.....	0.67	2	1.2	0.18	20	0.743	1.17	32
1991D.....	0.25	2	1.9	$\geq 1.52$	27	4.42	0.49	10
1999ex.....	0.30	2	0.9	0.25	19	0.967	1.05	71
Ic								
1962L.....	0.11	2	0.6	0.37	19	6.92E-3	0.85	11
1983I.....	0.33	3	0.7	0.23	17	0.140	0.46	18
1983V.....	0.99	2	1.3	0.15	19	3.25E-3	0.35	5
1987M.....	0.19	4	0.4	0.13	14	3.49E-3	0.72	4
1990B.....	0.55	2	0.9	0.14	18	0.229	1.08	26
1992ar.....	1.14	2	1.5	0.84	20	0.103	0.67	7
1994I.....	0.55	5	0.5	0.08	14	0.744	0.53	50
1997ef.....	3.26	6	3.1	0.16	23	0.491	0.23	22
1998bw.....	31.0	7	6.2	0.78	23	2.26	0.41	105
2002ap.....	2.72	8	1.7	0.14	19	1.50	0.23	60

REFERENCES.—For the  $E_k/M_{\text{ej}}$  relation: (1) Blinnikov et al. 1998; (2)  $E_k/M_{\text{ej}}$  was calculated as described in the text; (3) Shigeyama et al. 1990; (4) Nomoto et al. 1990; (5) Young et al. 1995; (6) Iwamoto et al. 2000; (7) Nakamura et al. 2001; (8) Mazzali et al. 2002.



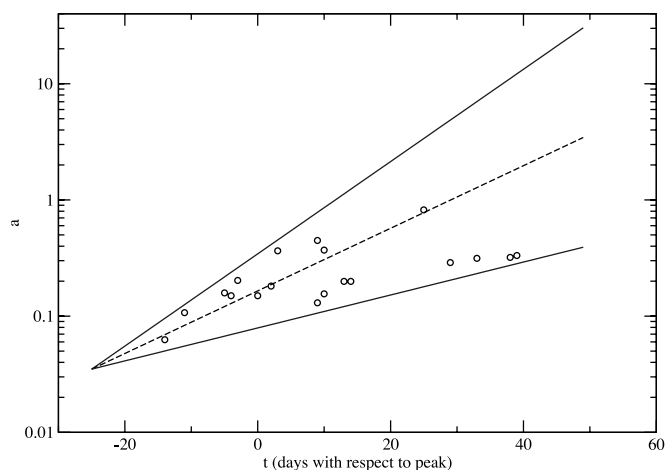


FIG. 9.—For normal SE SNe,  $a(t)$  on a log scale with solid lines showing the upper and lower limits and the dashed line showing the mean. [See the electronic edition of the Journal for a color version of this figure.]

difference between the dashed line and the solid lines is taken as the uncertainty. For the remaining events of the sample (those not having  $E_k/M_{\text{ej}}$  values from numerical LC calculations), we used Figures 9 and 10 with our estimates of  $v_{\text{phot}}(t)$  to obtain estimates of  $E_k/M_{\text{ej}}$ . With  $E_k/M_{\text{ej}}$  thus estimated spectroscopically, and three rather than four adjustable model parameters, we obtained relatively good fits with reasonable parameter values (in most cases).

### 3.3. Results

The parameter values determined from the best model fits are listed in Table 6. Because uncertainties are not available for each data point in all LCs, we quote the uncertainty at peak,  $\delta M_V$ , as the characteristic uncertainty. The uncertainties in  $M_V$  given in Table 6 differ from those listed in Tables 1–3 because here each one has the uncertainty in  $E_k/M_{\text{ej}}$  added in quadrature.

About half of the SNe modeled here have been modeled in similar studies; most by more sophisticated numerical models. Since our model is an analytic model, it has the advantage of being fast, and therefore, we can use it on a larger sample. Table 7 gives a comparison of our results to the results of the other studies. The values of  $M_{\text{ej}}$  from these other models tend to be larger than ours by a factor of approximately 2.

Since at least some, if not all, hypernovae are associated with GRBs, there is likely some interaction between the GRB jet and the expanding SN shell. A first-order approximation is to say that the SN occurs independently of the GRB. For our simple model this is a reasonable approximation.

#### 3.3.1. Type Ib

SN 1993J is the only SE SN that has been observed early enough to see the breakout shock in the  $V$ -band LC. Because the breakout shock has not been incorporated into the model we are using, that part of the LC has been omitted from our analysis. The model fit for SN 1993J (Fig. 11a), with  $E_k = 0.66$  foe and  $M_{\text{ej}} = 1.3 M_{\odot}$ , looks satisfactory, although  $\chi^2 = 2.14$  is somewhat large, probably due to the small adopted value of  $\delta M_V$ . Numerical LC calculations were carried out by Young et al. (1995) and Blinnikov et al. (1998); the former imposed  $E_k = 1$  foe and favored a model having  $M_{\text{ej}} = 2.6 M_{\odot}$ ; the latter adopted a model having  $E_k = 1.2$  foe and obtained a fit with  $M_{\text{ej}} = 2.45 M_{\odot}$ . If we impose  $E_k = 1$  foe and let  $M_{\text{ej}}$  vary, we get  $M_{\text{ej}} = 1.6 M_{\odot}$  (Table 7).

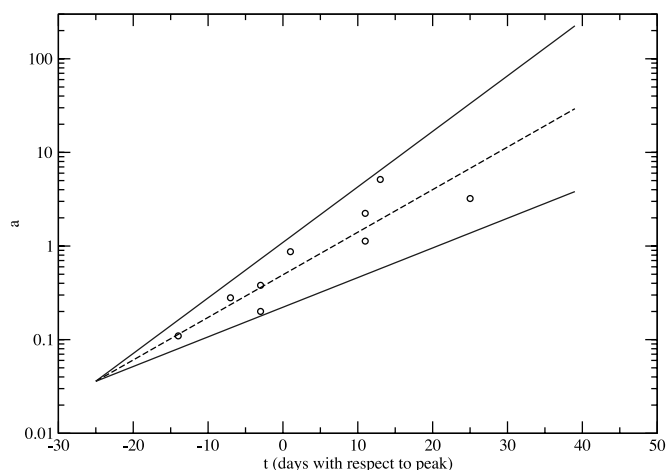


FIG. 10.—For hypernovae,  $a(t)$  on a log scale with solid lines showing the upper and lower limits and the dashed line showing the mean. [See the electronic edition of the Journal for a color version of this figure.]

The model fit for SN 1996cb (Fig. 11b), with  $E_k = 0.22$  foe and  $M_{\text{ej}} = 0.9 M_{\odot}$ , is slightly too dim at the peak, but overall it is satisfactory.

#### 3.3.2. Type Ib

Of the seven SNe Ib LCs plotted in Figure 3, five are worth fitting. The model fit to the fragmentary LC of SN 1983N (Fig. 12a), with  $E_k = 0.30$  foe and  $M_{\text{ej}} = 0.8 M_{\odot}$ , is good. We were not able to obtain an acceptable fit to the entire LC of SN 1984L (see Fig. 13b) because of the exceptionally slow decline in the tail (Fig. 3). However, when the data obtained later than 200 days after explosion were omitted, we did obtain a satisfactory fit (Fig. 12c), with  $E_k = 0.97$  foe and  $M_{\text{ej}} = 1.8 M_{\odot}$  (this result is denoted “pk” in Table 6). Baron et al. (1993) also had trouble fitting all of the data with detailed LC calculations and were forced to use what they regarded as an improbable model having a very small optical opacity and  $E_k \simeq 20$  foe,  $M_{\text{ej}} \simeq 50 M_{\odot}$ .

The LC of SN 1990I (Fig. 12d) drops rapidly after 250 days, and our best-fitting model, which has  $E_k = 0.67$  foe and  $M_{\text{ej}} = 1.2 M_{\odot}$ , cannot account for this. The problem with the fit near peak brightness is due to the compromise between trying to fit the tail and the peak. If the data later than 250 days are ignored, we get a better fit with only slight changes in the model parameters.

SN 1991D, the brightest SN in the sample, has an exceptional LC that declines rapidly from the peak, yet from its spectra we obtain  $E_k/M_{\text{ej}} = 0.13$  foe  $M_{\odot}^{-1}$ , the smallest value in the sample. The model cannot reconcile these contradictory aspects (Fig. 12e). It is possible to get a good fit if we drop the constraint on the  $E_k/M_{\text{ej}}$  ratio, but then we obtain  $E_k/M_{\text{ej}} = 8$  foe  $M_{\odot}^{-1}$ , which is inconsistent with the spectra. Benetti et al. (2002) used a semianalytical model to fit the LC of SN 1991D. They suggested this peculiar event may have been a SN Ia exploding inside the extended helium-rich envelope of a companion star. If this is correct then although SN 1991D must be regarded as Type Ib according to SN spectral classification, physically it may have more in common with SNe Ia.

SN 1999ex has very good coverage around the peak, but there are no data for the tail. The model fit, with  $E_k = 0.30$  foe and  $M_{\text{ej}} = 0.9 M_{\odot}$ , is satisfactory.

Other studies have looked at the LCs of SN 1983N (Shigeyama et al. 1990) and SN 1990I (Elmhamdi et al. 2004) assuming

TABLE 7  
RESULTS COMPARED TO OTHER STUDIES

SN	Study	$E_k$ (foe)	$M_{ej}$ ( $M_{\odot}$ )	Comments
I Ib				
1993J.....	This paper	0.66	1.3	
	This paper (impose $E_k = 1$ foe)	1	1.6	
	Young et al. (1995)	1	2.6	
	Blinnikov et al. (1998)	1.2	2.45	
I b				
1983N.....	This paper	0.30	0.8	No $^{56}\text{Ni}$ mixing
	This paper (impose $E_k = 1$ foe)	1	1.3	No $^{56}\text{Ni}$ mixing
	Shigeyama et al. (1990)	1	2.7	Extensive $^{56}\text{Ni}$ mixing
1990I.....	This paper	0.67	1.2	
	This paper (impose $E_k = 1$ foe)	1	1.4	
	Elmhamdi et al. (2004)	1	3.7	Late times only
I c				
1983I.....	This paper	0.33	0.7	No $^{56}\text{Ni}$ mixing
	This paper (impose $E_k = 1$ foe)	1	1.1	No $^{56}\text{Ni}$ mixing
	Shigeyama et al. (1990)	1	2.1	Extensive $^{56}\text{Ni}$ mixing
1987M.....	This paper	0.19	0.4	No $^{56}\text{Ni}$ mixing
	This paper (impose $E_k = 1$ foe)	1	0.8	No $^{56}\text{Ni}$ mixing
	Nomoto et al. (1990)	1	2.1	Extensive $^{56}\text{Ni}$ mixing
1997ef.....	This paper	3.3	3.1	
	Iwamoto et al. (2000)	8	7.6	
1998bw.....	This paper	31	6.2	
	Nakamura et al. (2001)	50	10	
	Woosley et al. (1999)	22	6.5	
2002ap.....	This paper	2.7	1.7	
	Mazzali et al. (2002)	4–10	2.5–5	

$E_k = 1$  foe. Their results are listed in Table 7 along with our results for comparison, as well as what we found when we imposed  $E_k = 1$  foe. In both cases our value for  $M_{ej}$  was somewhat smaller and was increased when imposing  $E_k = 1$  foe.

3.3.3. Type Ic

Model fits were carried out for all of the SN Ic LCs plotted in Figure 4 except for SN 1991N. The fit for the limited LC of SN 1962L, with  $E_k = 0.11$  foe and  $M_{ej} = 0.6 M_{\odot}$ , is satisfactory

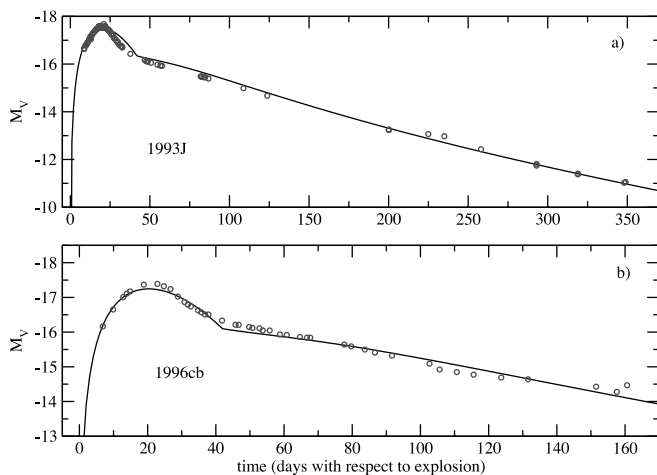


FIG. 11.—Best fit for the SNe I Ib (graphs are scaled independently). [See the electronic edition of the Journal for a color version of this figure.]

(Fig. 13a);  $M_{Ni} = 0.37$  is more than half as high as  $M_{ej}$ . The very low  $\chi^2$  is due to the large uncertainty of  $\delta M_V = 0.85$ .

For SN 1983I (Fig. 13b) there are no prepeak data. Our fit, with  $E_k = 0.33$  foe and  $M_{ej} = 0.7 M_{\odot}$ , is satisfactory. Our fit to the fragmentary LC of SN 1983V (Fig. 13c) is satisfactory, with  $E_k = 0.99$  foe and  $M_{ej} = 1.3 M_{\odot}$ . Our fit to the fragmentary LC of SN 1987M also is satisfactory (Fig. 13d), with  $E_k = 0.19$  foe and  $M_{ej} = 0.4 M_{\odot}$ .

The fit for SN 1990B (Fig. 13e), with  $E_k = 0.55$  foe and  $M_{ej} = 0.9 M_{\odot}$ , is quite good except for the last data point. According to Clocchiatti et al. (2001), that point is especially uncertain because of the difficulty in subtracting the host galaxy light. SN 1992ar is the brightest SN Ic in the sample. The model fit (Fig. 13f), with  $E_k = 1.1$  foe,  $M_{ej} = 1.5 M_{\odot}$ , and a high value of  $M_{Ni} = 0.84 M_{\odot}$ , is acceptable.

SN 1994I has a very narrow LC peak, and the best model fit (Fig. 14a), with  $E_k = 0.55$  foe and  $M_{ej} = 0.5 M_{\odot}$ , is too broad at peak. Thus, the value of  $t_{rise}$  given in Table 6, which already is the smallest value in the sample, is too large.

The last three LCs are those of three hypernovae. As mentioned above, these are SE SNe that have very broad, blueshifted absorption features at early times. The LC of SN 1997ef, which has a very broad peak and appears to have a very late transition point (Fig. 14b), is not well fitted by our model, which gives  $E_k = 3.3$  foe and  $M_{ej} = 3.1 M_{\odot}$ . The model fit for SN 1998bw (Fig. 14c), with  $E_k = 31$  foe and  $M_{ej} = 6.2 M_{\odot}$ , is good except near the transition point. This is by far the highest value of  $E_k$  for the events of the sample. Figure 14d shows the fit for SN 2002ap, with  $E_k = 2.7$  foe and  $M_{ej} = 1.7 M_{\odot}$ . Overall it is not bad, although the model peak is a bit dim, and the model transition point

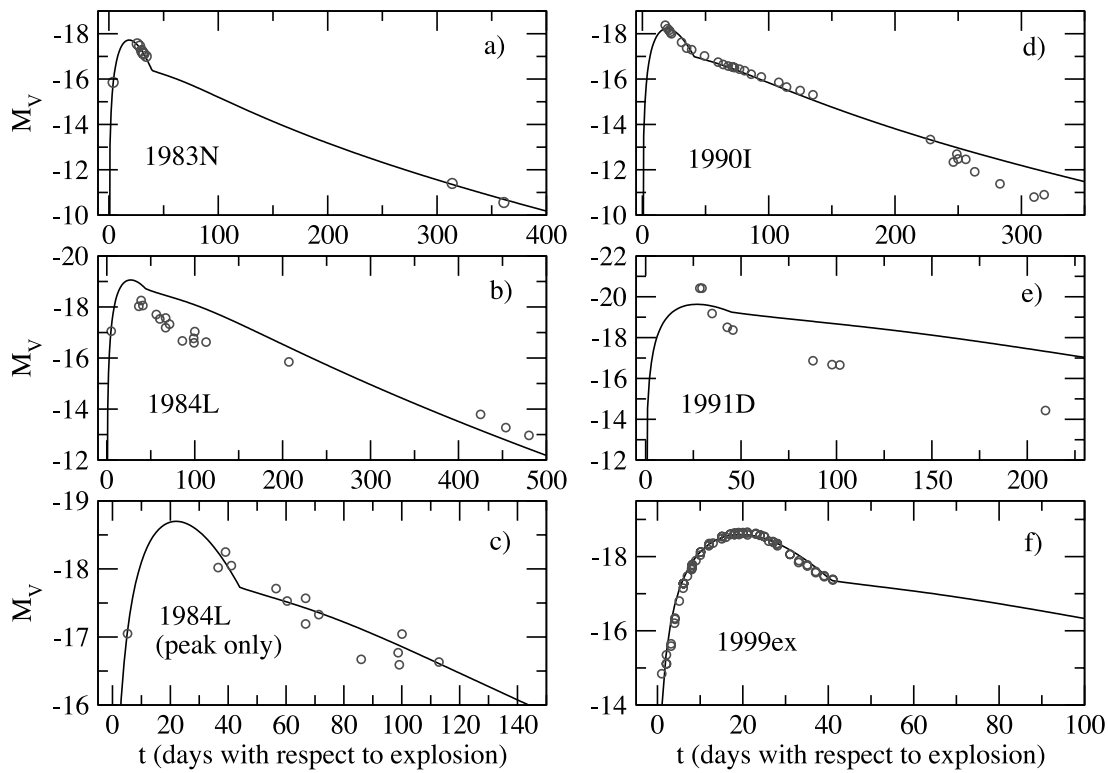


FIG. 12.—Best fit for the SNe Ib (graphs are scaled independently). [See the electronic edition of the Journal for a color version of this figure.]

is somewhat early. The model has trouble finding a tail that fits both the transition point and the two late-time data points.

Other studies have looked at the LCs of SN 1983I (Shigeyama et al. 1990) and SN 1987M (Nomoto et al. 1990) assuming  $E_k = 1$  foe. Their results are listed in Table 7 along with our

results for comparison, as well as what we found when we imposed  $E_k = 1$  foe. In both cases our value for  $M_{ej}$  was somewhat smaller but increased when imposing  $E_k = 1$  foe.

We compare our results for the three hypernovae with the results of other studies in Table 7. The value of  $E_k$  given in Table 6

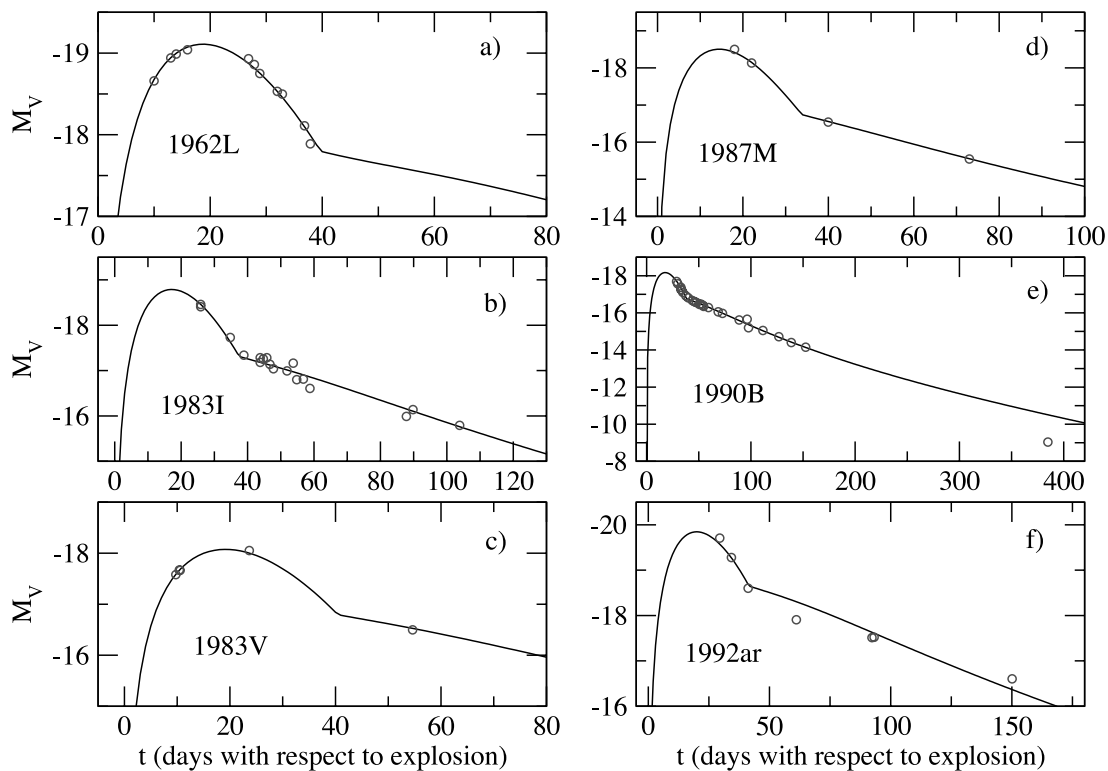


FIG. 13.—Best fit for SNe Ic (graphs are scaled independently). [See the electronic edition of the Journal for a color version of this figure.]

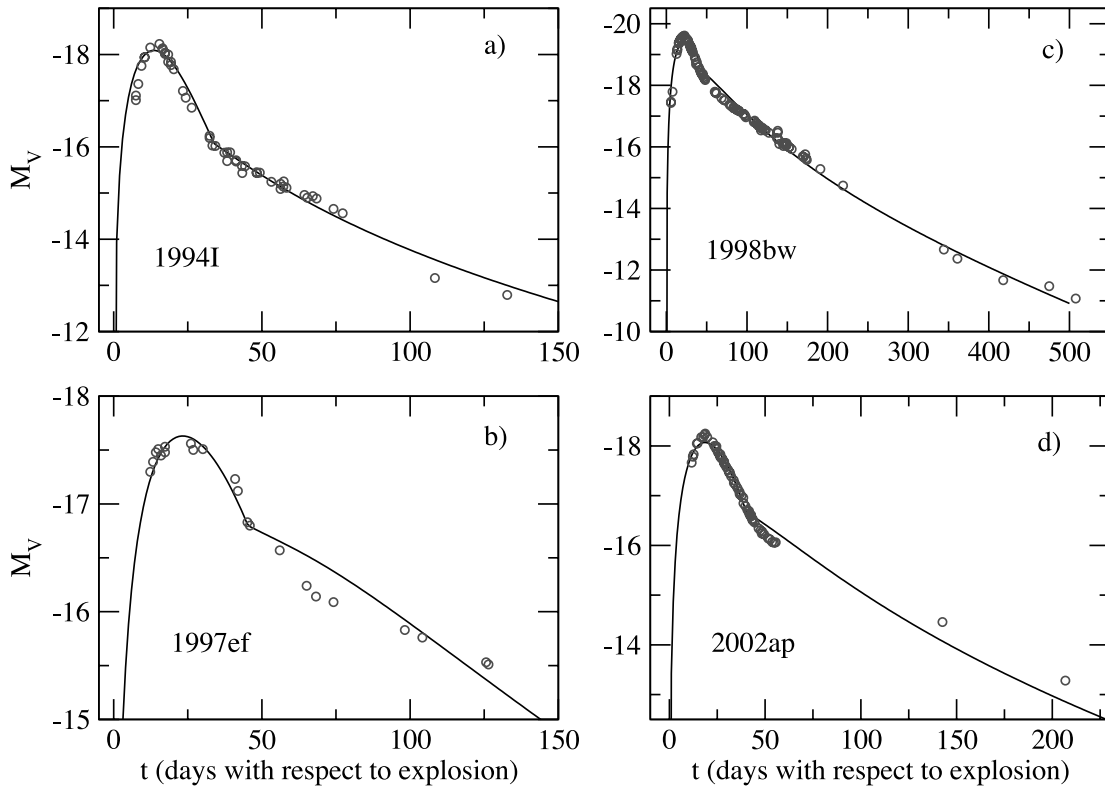


FIG. 14.—Best fit for more SNe Ic; (b) and (c) show hypernovae (graphs are scaled independently). [See the electronic edition of the Journal for a color version of this figure.]

for the brightest of the three (SN 1998bw) is comparable to the values found by Nakamura et al. (2001) ( $E_k = 50$  foe) and Woosley et al. (1999) ( $E_k = 22$  foe). The dimmest of the three hypernovae (SN 1997ef) is compared to a study by Iwamoto et al. (2000) in which they obtained  $E_k = 8$  foe and  $M_{ej} = 7.6 M_{\odot}$ .

#### 4. SUMMARY

We have used the available data to characterize the absolute magnitude distributions of the SE SNe in the current observational sample. Most SE SNe have a “normal” luminosity, which at  $M_V = -17.77 \pm 0.06$  is about a magnitude and a half dimmer than SNe Ia. One-sixth of the current sample of SE SNe are overluminous, i.e., more luminous than SNe Ia, but these are strongly favored by observational selection, so the true fraction of SE SNe that are overluminous is much lower than one-sixth. The small size of the sample and the considerable absolute magnitude uncertainties, especially those due to host galaxy extinction, still prevent an absolute magnitude difference between SNe Ib and Ic from being firmly established. Three of the four (or four of the five, counting SN 1999as) overluminous SE SNe are known to have had unusual spectra; a few of the normal-luminosity SE SNe also have had unusual spectra. Much more data on SE SNe are needed in order to better determine the absolute-magnitude distributions and to correlate absolute magnitudes with spectroscopic characteristics.

Absolute LCs in the  $V$  band (some fragmentary) are available for two SNe Iib, seven SNe Ib, and 12 SNe Ic, including three hypernovae. Two of the SNe Ib, SN 1984L and 1991D, have LCs that are quite different from those of the others. The LCs of the SNe Ic are rather diverse. The LC of SN 1994I, often considered to be a typical SN Ic, is actually the most rapidly declining LC in the SN Ic sample.

The simple analytical LC model was applied to two SNe Iib, five SNe Ib, and 10 SNe Ic. Instead of assuming a kinetic energy, such as the canonical 1 foe, an  $E_k/M_{ej}$  ratio was estimated on the basis of spectroscopy, and the model fits then produced internally consistent values of  $E_k$ ,  $M_{ej}$ , and  $M_{Ni}$ .

Reasonably good fits were obtained for the two SNe Iib and three of the five SNe Ib. The slowly decaying tail of the SN 1984L LC and the rapid decline from the peak of the SN 1991D LC cannot be fitted by the model. With the exception of the hypernova SN 1997ef, reasonable fits were obtained for the SNe Ic, with a considerable range in the parameter values. As expected, the hypernovae have high  $E_k$  and somewhat high  $M_{ej}$ , but only one of the three has high  $M_{Ni}$ .

Our values of  $M_{ej}$  (and  $E_k$ ) tend to be lower than those obtained by others by means of numerical LC calculations, while our values for  $M_{Ni}$  are a little higher. Some of the other numerical calculations are based on an assumed canonical value of  $E_k = 1$  foe. Because our spectroscopic constraint on  $E_k/M_{ej}$  together with our LC model leads to lower  $E_k$ , and lower  $E_k$  makes the LC peak dimmer, we need slightly higher  $M_{Ni}$  values to make the LC peaks as bright as observed.

The diversity among SN Ic LCs is of special interest in connection with the ongoing search for SN signals in GRB afterglows. In a forthcoming paper we will apply the same modeling technique used in this paper to the putative SN bumps in GRB afterglow LCs. This will enable us to infer internally consistent SN parameter values for comparison with the results of this paper, and to investigate the issue of whether the GRBs and the associated SNe are coincident in time or whether, as in the supernova model, the SN precedes the gamma-ray burst.

We would like to thank Rollin C. Thomas for helpful comments and suggestions. Support for this work was provided by NASA through grants GO-09074 and GO-09405 from the Space Telescope Science Institute, which is operated by the Association

of Universities for Research in Astronomy, Inc., under NASA contract NAS5-25255. Additional support was provided by National Science Foundation grants AST 99-86965 and AST 02-04771.

## REFERENCES

- Arnett, D. 1980, *ApJ*, 237, 541  
 ———. 1982, *ApJ*, 253, 785  
 Ayani, K., Furusho, R., Kawakita, H., Fujii, M., & Yamaoka, H. 1999, *IAU Circ.* 7244  
 Barbon, R., Benetti, S., Cappellaro, E., Pata, F., Turatto, M., & Iijima, T. 1995, *A&AS*, 110, 513  
 Barbon, R., Buondi, V., Cappellaro, E., & Turatto, M. 1999, *A&AS*, 139, 531  
 Baron, E., Young, T., & Branch, D. 1993, *ApJ*, 409, 417  
 Barth, A. J., van Dyk, S., Filippenko, A., Leibundgut, B., & Richmond, M. 1996, *AJ*, 111, 2047  
 Benetti, S., Branch, D., Turatto, M., Cappellaro, E., Baron, E., Zampieri, L., Della Valle, M., & Pastorello, A. 2002, *MNRAS*, 336, 91  
 Benetti, S., Cappellaro, E., Turatto, M., & Pastorello, A. 2000, *IAU Circ.* 7375  
 Bertola, F. 1964, *Ann. Astrophys.*, 27, 319  
 Blinnikov, S., Eastman, R., Bartunov, O., Popolitov, V., & Woosley, S. 1998, *ApJ*, 496, 454  
 Branch, D. 2003, in *IAU Symp.* 212, *A Massive Star Odyssey, from Main Sequence to Supernova*, ed. K. A. van der Hucht, A. Herrero, & C. Estaban (San Francisco: ASP), 346  
 Branch, D., et al. 2002, *ApJ*, 566, 1005  
 Clocchiatti, A., Wheeler, J. C., Benetti, S., & Frueh, M. 1996, *ApJ*, 459, 547  
 Clocchiatti, A., et al. 1997, *ApJ*, 483, 675  
 ———. 2000, *ApJ*, 529, 661  
 ———. 2001, *ApJ*, 553, 886  
 Drozdovsky, I., Schulte-Ladbeck, R., Hopp, U., Greggio, L., & Crone, M. 2002, *AJ*, 124, 811  
 Elmhamdi, A., Danziger, I. J., Cappellaro, E., Della Valle, M., Gouiffes, C., Phillips, M. M., & Turatto, M. 2004, *A&A*, 426, 963  
 Feldmeier, J., Ciardullo, R., & Jacoby, G. 1997, *ApJ*, 479, 231  
 Filippenko, A. 1987, *IAU Circ.* 4428  
 ———. 1988, *AJ*, 96, 1941  
 Filippenko, A., Porter, A., & Sargent, W. 1990, *AJ*, 100, 1575  
 Foley, R., et al. 2003, *PASP*, 115, 1220  
 Freedman, W., et al. 2001, *ApJ*, 553, 47  
 Galama, T., et al. 1998, *Nature*, 395, 670  
 ———. 1999, *A&AS*, 138, 465  
 Gal-Yam, A., Ofek, E., & Shemmer, O. 2002, *MNRAS*, 332, L73  
 Garnavich, P., Matheson, T., Olszewski, E. W., Harding, P., & Stanek, K. Z. 2003, *IAU Circ.* 8114  
 Grothues, H. G., & Schmidt-Kaler, T. 1991, *A&A*, 242, 357  
 Hamuy, M., et al. 2002, *AJ*, 124, 417  
 Hatano, K., Branch, D., Nomoto, K., Deng, J. S., Maeda, K., Nugent, P., & Aldering, G. 2001, *BAAS*, 198, 39.02  
 Homeier, N. L. 2005, *ApJ*, 620, 12  
 Iwamoto, K., et al. 2000, *ApJ*, 534, 660  
 Jeffery, D. 1999, preprint (astro-ph/9907015)  
 Jha, S., Garnavich, P., Challis, P., & Kirshner, R. 1998, *IAU Circ.* 7011  
 Kantowski, R., Kao, J., & Thomas, R. C. 2000, *ApJ*, 545, 549  
 Kinugasa, K., et al. 2002, *ApJ*, 577, L97  
 Klose, S., Guenther, E., & Woitas, J. 2002, *GRB Circ.*, 1248, 1  
 Korth, S. 1991a, *IAU Circ.* 5234  
 ———. 1991b, *IAU Circ.* 5251  
 Krisciunas, K., & Rest, A. 2000, *IAU Circ.* 7382  
 Leibundgut, B., Phillips, M. M., & Graham, J. A. 1990, *PASP*, 102, 898  
 Leibundgut, B., Tammann, G. A., Cadonau, R., & Cerrito, D. 1991, *A&AS*, 89, 537  
 Lewis, J., et al. 1994, *MNRAS*, 266, L27  
 Matheson, T., Filippenko, A., Chornock, R., Leonard, D., & Li, W. 2000, *AJ*, 119, 2303  
 Matheson, T., Filippenko, A., Li, W., Leonard, D., & Shields, J. 2001, *AJ*, 121, 1648  
 Maza, J., & Ruiz, M. T. 1989, *ApJS*, 69, 353  
 Mazzali, P., Iwamoto, K., & Nomoto, K. 2000, *ApJ*, 545, 407  
 Mazzali, P., et al. 2002, *ApJ*, 572, L61  
 McKenzie, E., & Schaefer, B. 1999, *PASP*, 111, 964  
 Nakamura, T., Mazzali, P., Nomoto, K., & Iwamoto, K. 2001, *ApJ*, 550, 991  
 Nomoto, K., Filippenko, A., & Shigeyama, T. 1990, *A&A*, 240, L1  
 Pandey, F., Anupama, G., Sagar, R., Bhattacharya, D., Sahu, D., & Pandey, J. 2003, *MNRAS*, 340, 375  
 Phillips, M. M., & Graham, J. A. 1984, *IAU Circ.* 3946  
 Phillips, M., & Hamuy, M. 1992, *IAU Circ.* 5574  
 Porter, A., & Filippenko, A. 1987, *AJ*, 93, 1372  
 Qiu, Y., Li, W., Qiao, Q., & Hu, J. 1999, *AJ*, 117, 736  
 Richardson, D., Branch, D., Casebeer, D., Millard, J., Thomas, R. C., & Baron, E. 2002, *AJ*, 123, 745 (R02)  
 Richmond, M., Treffers, R., Filippenko, A., Paik, Y., Leibundgut, B., Schulman, E., & Cox, C. 1994, *AJ*, 107, 1022  
 Richmond, M., et al. 1996, *AJ*, 111, 327  
 Saha, A., Sandage, A., Tammann, G. A., Dolphin, A. E., Christensen, J., Panagia, N., & Macchetto, F. D. 2001, *ApJ*, 562, 314  
 Schaefer, B. 1995, *ApJ*, 450, L5  
 ———. 1996, *ApJ*, 464, 404  
 Schlegel, D., Finkbeiner, D., & Davis, M. 1998, *ApJ*, 500, 525  
 Shigeyama, T., Nomoto, K., Tsujimoto, T., & Hashimoto, M. 1990, *ApJ*, 361, L23  
 Sollerman, J., Kozma, C., Fransson, C., Leibundgut, B., Lundqvist, P., Ryde, F., & Woudt, P. 2000, *ApJ*, 537, L127  
 Stritzinger, M., et al. 2002, *AJ*, 124, 2100  
 Thim, F., Tammann, G. A., Saha, A., Dolphin, A., Sandage, A., Tolstoy, E., & Labhardt, L. 2003, *ApJ*, 590, 256  
 Tsvetkov, D. 1985, *AZh*, 62, 365  
 ———. 1994, *Astron. Rep.*, 38, 74  
 Tully, R. B. 1988, *Nearby Galaxies Catalog* (Cambridge: Cambridge Univ. Press)  
 Turatto, M., Benetti, S., & Cappellaro, E. 2003, in *From Twilight to Highlight: The Physics of Supernovae*, ed. W. Hillebrandt & B. Leibundgut (Berlin: Springer), 200  
 van Driel, W., et al. 1993, *PASJ*, 45, L59  
 Wellmann, P., & Beyer, M. 1955, *Z. Astrophys.*, 35, 205  
 Wheeler, J. C., & Levreault, R. 1985, *ApJ*, 294, L17  
 Woosley, S., Eastman, R., & Schmidt, B. 1999, *ApJ*, 516, 788  
 Yoshii, Y., et al. 2003, *ApJ*, 592, 467  
 Young, T., Baron, E., & Branch, D. 1995, *ApJ*, 449, L51